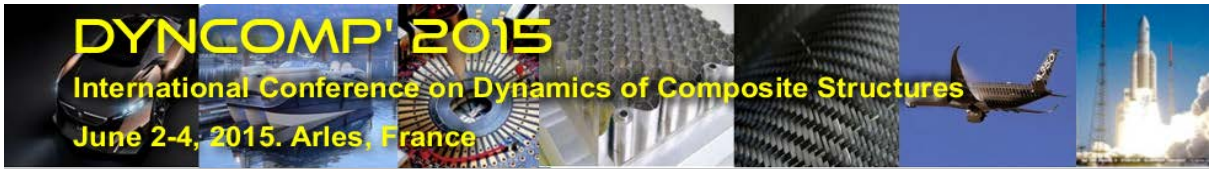


# A NEW LAMINATE MODEL FOR BROADBAND FREQUENCY ANALYSIS

Gérard Borello

InterAC
10 impasse Borde-Basse, Z.A. La Violette, 31240 L'Union, FRANCE
gerard.borello@interac.fr

## ABSTRACT

*For predicting vibratory responses of multi-layered panels over a wide frequency range (100-10000 Hz), a new laminate theory has been developed. It overcomes the limit of classical zigzag laminate theory reached when panels start to undertake transverse resonant behavior. This theory mixes the three degrees of freedom ($u_0$, $v_0$, $w_0$) of the thin orthotropic panel, statically equivalent to the layup assembly with the three "blocked" degrees of freedom ($u_i$, $v_i$, $w_i$) of each layer, considered in relative motion to ($u_0$, $v_0$, $w_0$). A panel made of N layers is thus described by 3(N+1) displacement variables coupled by a dynamic operator obtained by assembling plate, cylinder or doubly-curved shell thin orthotropic dynamical operators of individual layers depending on geometry. The real coupled operator is first analytically solved for all possible (m, n) quantic numbers to get eigenvalues and eigenmodes from which is derived the modal density of flexural, shear and extensional modes. In a second time, all material properties are made complex and the operator is solved again to predict the frequency band-averaged mean damping loss factor of the assembly from the complex eigenvalues. Examples of modeling aerospace sandwich or sandwich with thin viscoelastic core are discussed against related FEM models. This theory adds a new class of SEA subsystems to SEA+ software, extending its modeling capability in addition to the introduction of an "extended orthotropic" material described by frequency dependent elastic constants.*

## 1 INTRODUCTION

Thin multi-layered elastic shells are components of many industrial products from spacecraft with light honeycomb sandwich panels to car dashboards made of stamped viscoelastic steel sheets. Their equivalent damping properties are needed for controlling the accuracy of statistical Energy Analysis (SEA) prediction of their vibroacoustic behavior as well as their modal density. Due to limitation of the classical laminate theory in the high frequency range (HF), a new method has been developed for deriving the coupled equations of multilayered shells considered as an assembly of 2D thin layers. This theory has been implemented in the SEA+ software and is briefly exposed in this document with some validation results.

## 2 DYNAMICAL DESCRIPTION OF INDIVIDUAL LAYERS

In HF, each elastic layer will asymptotically oscillate on its uncoupled $\{u_k, v_k, w_k\}$ displacement in respectively x, y and z axis, with (x, y) defining the plane of the layer.
$\{u_k, v_k, w_k\}$ are the local degrees of freedom of a layer k. The elastic behavior of layer neutral fiber is assumed to be orthotropic within (x, y) plane and defined by the following $E_{ij}$ matrix relating torque at neutral fiber to strains.

$$\begin{bmatrix} \sigma_{xx} \\ \sigma_{yy} \\ \sigma_{xy} \\ \sigma_{zz} \\ \sigma_{z\langle xy\rangle} \end{bmatrix} = \begin{bmatrix} E_x & \nu_x E_y & 0 & 0 & 0 \\ \nu_x E_y & E_x & 0 & 0 & 0 \\ 0 & 0 & G_{xy} & 0 & 0 \\ 0 & 0 & 0 & E_z & 0 \\ 0 & 0 & 0 & 0 & G_z \end{bmatrix} \begin{bmatrix} \varepsilon_{xx} \\ \varepsilon_{yy} \\ \gamma_{xy} \\ \varepsilon_{zz} \\ \langle \gamma_{zx}, \gamma_{zy} \rangle \end{bmatrix}$$

The two additional elastic parameters $E_z$ and $G_z$ are added for more flexibility in modeling complex design material. $C_{ij}$ coefficients are relating the corresponding forces applied to neutral fiber to displacement vector $\{u_k, v_k, w_k\}$ and its spatial derivatives by integrating previous stresses defined by $E_{ij}$ over the layer thickness.
The dynamic of a single layer is then described by its local 3x3 dynamic stiffness operator which applies to $\{u_k, v_k, w_k\}$ with expression given here for a flat thin layer:

$$L_k = \begin{bmatrix} C_{11}\partial''_{x^2} + C_{66}\partial''_{y^2} & (C_{12}+C_{66})\partial''_{xy} & 0 \\ (C_{12}+C_{66})\partial''_{xy} & C_{66}\partial''_{x^2} + C_{22}\partial''_{y^2} & 0 \\ 0 & 0 & D_{11}\partial^{(4)}_{x^4} + D_{22}\partial^{(4)}_{y^4} + 2(D_{12}+2D_{66})\partial^{(4)}_{x^2y^2} \end{bmatrix} \quad (2.1)$$

## 3 DYNAMICAL DESCRIPTION OF GLOBAL LAYER

When assembling the layers on top of each other, three complementary DoFs are added, $\{u_0, v_0, w_0\}$ for describing the low frequency motion when all layers are vibrating in phase with no relative motion between them as shown in Figure **1**.

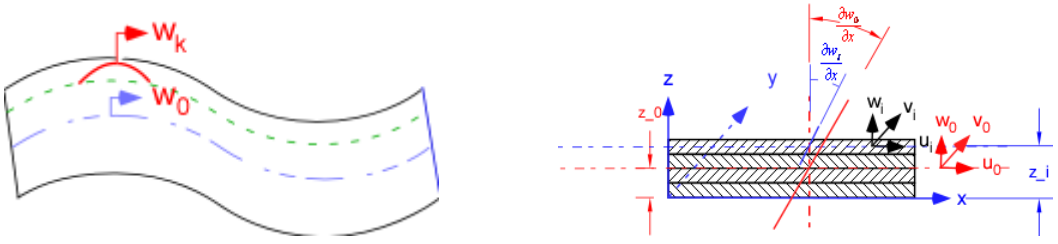


Figure 1. Degree of freedom of the laminate assembly

This global layer is assumed to behave as the equivalent "static" shell with $C_{ij}$ elastic matrix calculated for phased translational and rotational motions of all layers. Given $z_k$, the relative height of neutral fiber of a layer k vs $z_0$, fiber height of layer 0, the actual displacement vector $X$ of a layer k is expressed in the axis of global layer 0 as follows:

$$X = \begin{bmatrix} u(z,x,y,t) \\ v(z,x,y,t) \\ w(z,x,y,t) \end{bmatrix} = \begin{bmatrix} u_0(x,y,t) - z\dfrac{\partial w_0}{\partial x} \\ v_0(x,y,t) - z\dfrac{\partial w_0}{\partial y} \\ w_0(x,y,t) \end{bmatrix} H_{t_0}(z) + \begin{bmatrix} u_k(x,y,t) - (z-z_k)\dfrac{\partial w_k}{\partial x} \\ v_k(x,y,t) - (z-z_k)\dfrac{\partial w_k}{\partial y} \\ w_k(x,y,t) \end{bmatrix} H_{t_k/2}(z-z_k) = X_0 + X_k$$

H is the Heaviside function, indicating the motion of each layer is limited to its thickness.
Its dynamic stiffness is given by (2.1) using equivalent static $C_{ij(k)}$ coefficients.

## 4 COUPLING SCHEME OF GLOBAL AND LOCAL LAYERS

When excited by broadband random force, the layers will progressively decouple and will start to have relative motion between them. Assuming all layers will oscillate with common spatial phase function $g\psi$ , their vectorial motion is then given by:

$$X = \begin{bmatrix} U \\ V \\ W \end{bmatrix} g(x_0, y_0)\psi(z)e^{j\omega t} \tag{4.1}$$

$\psi(z)$ is assumed continuous along transverse section with continuity of displacement at layer interface but its derivative $\dfrac{\partial \psi}{\partial z}$ is discontinuous. $\dfrac{\partial \psi}{\partial z}$ is a distribution with derivative jumps $\theta_k$ at layer interfaces.

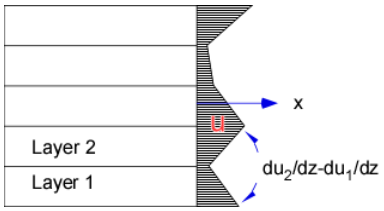


$\dfrac{\partial \psi}{\partial z}$ may then be expressed as:

$$\frac{\partial \psi}{\partial z} = \sum_k \theta_k(x,y)(\delta_k(z-z_k) + \left\{\frac{\partial \psi}{\partial z}(x,y,z\right\}$$

$\{\ \}$ means $\dfrac{\partial \psi}{\partial z}$ is continuous outside discontinuity interval.

Derivative jump is then estimated by $\theta_{k(k-1)} = \dfrac{\psi(z_k) - \psi(z_{k-1})}{z_k - z_{k-1}}$ which means interlayer forces will be proportional to the difference of their $\psi(z_k)$ motion amplitude.

The general coupling scheme of global and local layer is sketched in Figure **2** as a generalized mass-spring dynamic system where $X$ are vectors with components $\{u, v, w\}$ and stiffness terms are 3x3 dynamic operators. As well as mass operator, $L_k$ is the dynamic operator of a layer k coupled through springs to global layer described by $L_0$. To write down the coupled equations of the system, we have to provide expression of the coupled springs between global and local layers and between local layers.

The spring operator $L_{k0}$ represents the various elastic forces connecting local and global layers.

$L_{k0}$ is split into two additive terms: first term $L_{k0(x,y)}$ is calculated from the strain energy due to the joint work of their respective dynamic operators $L_k$ and $L_0$. Effectively, a k-layer when

moving is developing work within the stress field generated by $L_0$. The work $E$ is thus computed from $E = \sum_k \int_{t_k} (\sigma_k + \sigma_0)(\varepsilon_k - \varepsilon_0)^* d\varepsilon_k$ representing the relative work of all motions $X_k$. Second term $I_{k0(z)}$ corresponds to work induced by complementary stresses generated by $\psi(z)$ strain and not accounted in the work related to $L_{k0(x,y)}$. They are introduced as complementary stiffness matrix added to $I_{k0(x,y)}$ as the two types of stresses are acting in parallel.

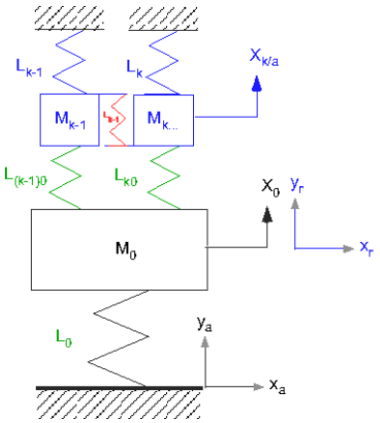


Figure 2. The global-to-local coupling scheme

The coupling between two adjacent layers k and k-1 is described by the matrix $I_{k(k-1)}$ of which components are springs acting on the various layer motions. For example, along z-axis, layers may be compressed with a related interface stress $\sigma_{zz}$. Assuming a continuous linear compression strain at interfaces A and B, potential energy is given by:

$$U = \frac{1}{2}\left\{K_{zz-}\left(w_k - w_{k-1}\right)^2 + K_{zz+}\left(w_k - w_{k+1}\right)^2\right\}$$

If the stiffness $K_{zz}$ is calculated between the respective neutral fibers of two adjacent layers, it may be calculated following:

$$K_{zz-} = \frac{K_{zz}^{(k-1)} K_{zz}^{(k)}}{K_{zz}^{(k-1)} + K_{zz}^{(k)}} \qquad K_{zz+} = \frac{K_{zz}^{(k+1)} K_{zz}^{(k)}}{K_{zz}^{(k+1)} + K_{zz}^{(k)}} \qquad K_{zz}^{(k)} = \beta E_{ZZ} / t_k$$

The parameter $\beta$ is depending on chosen $g(x_0, y_0)$ function, $K_{zz}$ being defined as a stiffness per unit m², proportional to $\frac{1}{A}\int_{x,y} g(x,y)$.

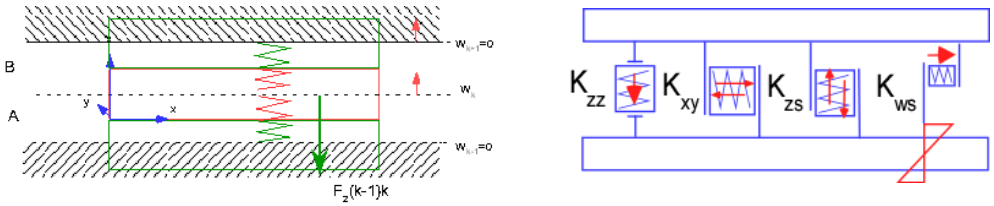


Figure 3. **Left**: Sketch for z-stiffness term derivation of $K_{zz}$ impedance - **Right**: the four coupling impedances introduced in the laminate model

Similarly, there are shear forces at interfaces when rotation $\frac{\partial \psi}{\partial z}$ is non-zero. Four different springs, $K_{zz}$, $K_{xy}$, $K_{xyz}$ and $K_{ws}$ are then acting in the motion $X_k$ when all other layers are blocked at their neutral fibers.

$K_{xy}$ is the shear spring due to rotation $\frac{\partial \psi}{\partial z}$ and calculated as:

$$K_{xy} = \frac{K_{xy}^{(k-1)} K_{xy}^{(k)}}{K_{xy}^{(k-1)} + K_{xy}^{(k)}} \text{ with } K_{xz}^{k} = \frac{\beta G_{zz}}{t}$$

The related force applied in the plane *(x, y)* is given by:

$$F_{xy} = -K_{xy}\left(u_k - u_{k-1}\right)$$

$F_{xy}$ corresponds to the stress $\sigma_{zx}$ or $\sigma_{zy}$ and sketched as force $S_{xz(k-1)k}$ in next figure.

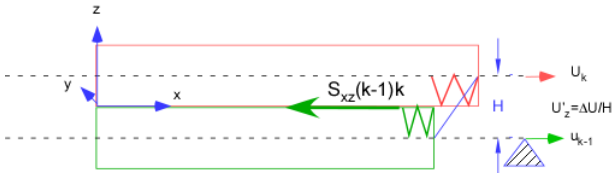


$K_{xyz}$ and $K_{ws}$ are respectively due to moment generated by $F_{xy}$ when motion is expressed at neutral fiber. The second derivative of this moment gives two shear forces in the transverse section (*x*, *z*) and (*y*, *z*) which opposes to inertial force and act of *w* components and due to the moment of $F_{xy}$ and the moment exerted by the rotation of the section of layer k ($K_{ws}$ stiffness). A last stiffness term is introduced. This stiffness is due to differential rotation $\left(\frac{\partial w_k}{\partial x} - \frac{\partial w_{k-1}}{\partial x}\right)$ inducing shear stress in (*x*, *z*) and (*y*, *z*) transverse planes, acting on *w's* components of motion.

## 5 SOLVING THE DYNAMICAL MATRIX

From previously defined set of interacting forces, the coupled equations of the multilayered motion are reduced to a set of linear relationships given in matrix form (given for two layers herbelow):

$$\begin{bmatrix} L_0 + L_{10} + L_{20} & -L_{10} & -L_{20} \\ -L_{10} & L_1 + L_{10} + L_{12} & -L_{12} \\ -L_{20} & -L_{12} & L_2 + L_{20} + L_{12} \end{bmatrix} \begin{bmatrix} X_0 \\ X_1 \\ X_2 \end{bmatrix} + \omega^2 \mathbf{M} \mathrm{X} = 0 \qquad (5.1)$$

Equations are next expressed in function of the relative local motion of layers k, $\delta X_k$.

Given $\delta X_k = X_k - X_0$, (5.1) becomes:

$$\begin{bmatrix} L_0 & -L_{10} & -L_{20} \\ L_1 & L_1 + L_{10} + L_{12} & -L_{12} \\ L_2 & -L_{12} & L_2 + L_{20} + L_{12} \end{bmatrix} \begin{bmatrix} X_0 \\ \delta X_1 \\ \delta X_2 \end{bmatrix} + \omega^2 \tilde{\mathbf{M}} \begin{bmatrix} X_0 \\ \delta X_1 \\ \delta X_2 \end{bmatrix} = 0 \qquad (5.2)$$

This matrix makes the dynamic problem easier to solve as the high-valued terms on the diagonal of $L_0$ are removed leading to more stability in the LF range where $L_0$ operator is predominant.

In relative motion, the mass matrix is non-diagonal and is given by:

$$\tilde{M} = \begin{bmatrix} M_0 & 0 & .. & .. & .. & 0 \\ M_1 & M_1 & 0 & 0 & .. & 0 \\ .. & .. & .. & .. & .. & 0 \\ M_k & 0 & 0 & M_k & 0 & 0 \\ .. & .. & .. & .. & .. & 0 \\ M_N & 0 & 0 & 0 & 0 & M_N \end{bmatrix}$$

To get a fast analytical solution, displacements in the (*x, y*) plane are constrained to some global shape compatible with boundary conditions such as:

$$g(x,y) = \sin\frac{m\pi x}{L_x}\sin\frac{n\pi y}{L_y} \text{ in case of simply supported edges.}$$

When applying the differential operators to $g(x,y)$, $\tilde{L}$ and $\tilde{M}$ matrices are becoming functions of quantic *m* and *n* numbers. For each pair (*m, n*), an eigenvalue problem is solved, leading, for N assembled layers, to a system of 3x(N+1) eigenvalues, $\lambda_{imn}$. After extraction, $\lambda_{imn}$ are sorted into extensional, shear and bending categories by analyzing the relative importance of eigenvector amplitudes in each *u, v, w* directions.

Finally, the band-averaged modal density and the band-averaged wavenumber are estimated from the set of all discrete $\lambda_{imn}$ up to some maximal *m, n* orders limited by the upper frequency of calculation.

The model is made more general by introducing frequency-dependent elastic parameters using *SEA+ Extended Material* definition.

The full dynamic matrix is then solved twice, the first solve giving the primary solution frequency and the second solve providing the final frequency after interpolating elastic matrix at primary solution frequency.

Modal damping loss factor (DLF) is estimated by transforming $\tilde{L}$ matrix into a complex matrix $\mathsf{L}$ using complex $C_{ij}$ matrix of which component related to each layer k are given by:

$$\tilde{C}ij_k = (1 + j\eta_k)\,Cij_k$$

with $\eta_k$ the local material damping associated to each layer.

The mean DLF of the assembly is finally delivered in integrated band format of width $\Delta\omega$ and central frequency $\omega_c$:

$$\langle \eta(\omega_c) \rangle_{\Delta\omega} = \frac{1}{N_{\Delta\omega}} \left\{ \sum_i X_i^T \,\mathrm{Im}\{\mathsf{L}\}\, X_i \Big/ \sum_i X_i^T \,\mathrm{Re}\{\mathsf{L}\}\, X_i \right\}$$

where $N_{\Delta\omega}$ is the number of eigenvalues retained in $\Delta\omega$ and $X_i$ eigenvector related to $\lambda_{imn}$.

## 6 APPLICATION TO VARIOUS SYSTEMS

### 6.1 Consistency of the formulation

The self-consistency of the formulation is checked against the calculation of an arbitrary isotropic thin plate of uniform material but decomposed into different number of layers for unchanged total thickness. A 1 m x 1 m uniform plate of 4-mm aluminum thickness is then modeled as SEA+ dynamic laminate plate with selected thickness distribution defined in next table.

| Case | Type | #Layer | t1 (mm) | t2 (mm) | t3 (mm) | t4 (mm) | t5 (mm) | Total t mm |
|---|---|---|---|---|---|---|---|---|
| P0 | uniform | 1 | 4 | | | | | 4 |
| P1 | Laminate | 1 | 4 | | | | | 4 |
| P2 | Laminate | 2 | 2 | 2 | | | | 4 |
| P3 | Laminate | 3 | 1 | 0.5 | 2.5 | | | 4 |
| P4 | Laminate | 4 | 1 | 1 | 1 | 1 | | 4 |
| P5 | Laminate | 5 | 1.5 | 1 | 0.25 | 1 | 0.25 | 4 |

Table 1. Consistency test of the formulation modeling same plate with different dynamic laminate settings (P0 is the reference plate result modeled as 4-mm uniform SEA+ plate)

Figure **4** shows all models are given same eigenfrequencies, modal density and mass except out of resonances where modal density is interpolated differently between uniform and laminate modeling.

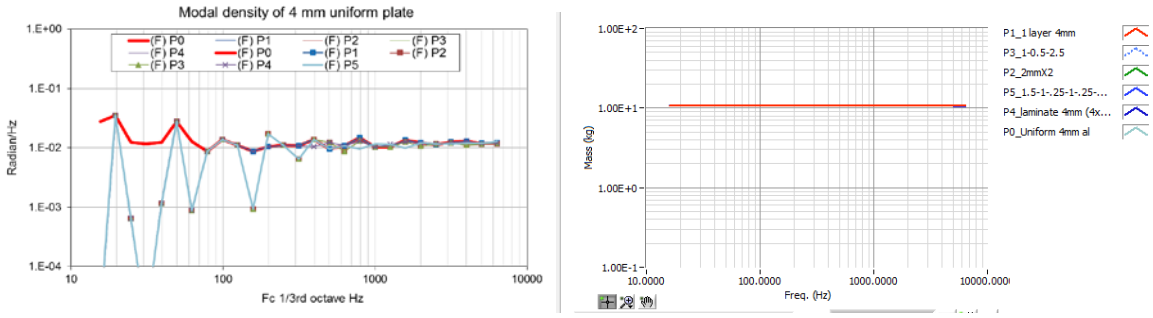


Figure 4. **Left**: modal density of 4mm-Al plate modeled as uniform and as dynamic laminate with different thickness distributions - **Right**: related mass of all plates

### 6.2 Aerospace sandwich flat plate structure

Case C1 is a 1 x 1 m² flat plate made of sandwich construction with two 1-mm aluminum skins and 10-mm NIDA core with G = 200 MPa, E = 3MPa and $\rho_c$ = 60 kg/m$^3$.

SEA+ calculation is compared with three FEM simulations with NASTRAN NX solver.

- ***C1 "PSOLID1"*** FEM model, skins are modeled using 2D-plate elements and glued to the core meshed with 3D-PSOLID elastic elements. PSOLID1 is simply-supported on edge of only one skin.
- ***C1 "PSOLID2"*** FEM model, same model than PSOLID1 but simply-supported on edges of the two skins.
- ***C1 "PCOMP"*** FEM model, both skins and core are modeled with 2D PCOMP plate laminate elements within a single 2D-plate and with simply-supported edges.

Real eigenmodes are extracted from FEM models by NASTRAN NX SOL103 solver and imported in SEA+ Virtual SEA solver [1] [2] [3] [4] to calculate related SEA parameters: modal density, wavenumber and mean input mobility. They are then compared to corresponding SEA+ Dynamic Laminate outputs. Figure **5** and Figure **6** show good agreement between SEA and both PCOMP and PSOLID FEM models for modal density and conductance (real part of driving point mobility). Mid to high frequency slopes of both flexural modal density and mobility spectra due to core shear are well-reproduced by SEA+ model. Shifting from PCOMP to PSOLID FEM models increases the first resonance frequencies provided by PCOMP. This is observed in the two selected boundary conditions: constraining one skin, then, two skins to simply-supported on edge, demonstrating the difficulty in predicting deterministic resonance frequencies even on simple systems.

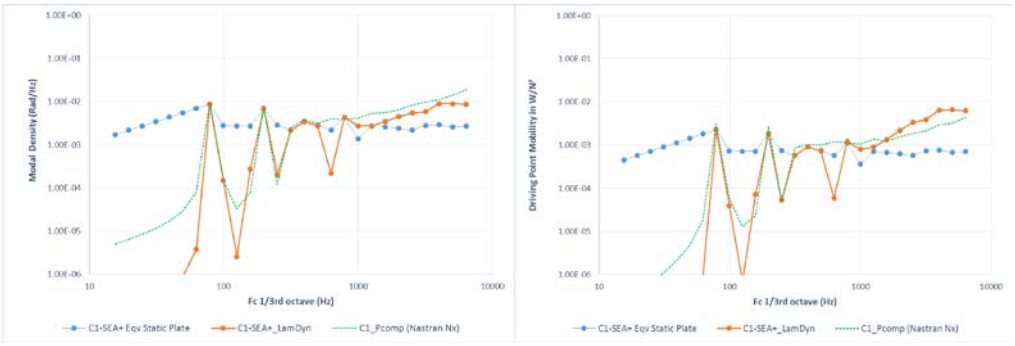


Figure 5. Case C1-Comparisons of (**Left**) Model density and (**Right**) conductance using SEA+ Dynamic Laminate (red), PCOMP NASTRAN (dashed green) and SEA+ uniform equivalent static plate (dot blue)

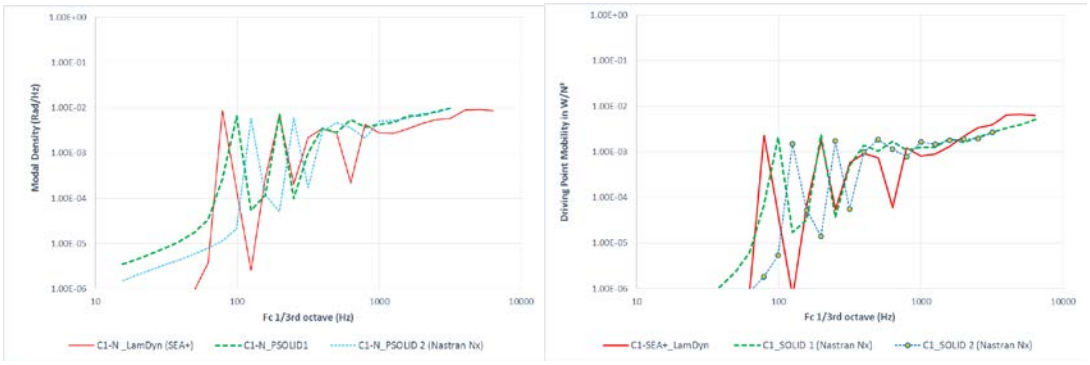


Figure 6. Case C1 - Comparisons of (**Left**) Model density and (**Right**) conductance using SEA+ Dynamic Laminate (red) and PSOLID 1 & 2 NASTRAN

### 6.3 Aerospace sandwich singly-curved structure

Case C2 is a quarter of cylinder in same sandwich than C1. Radius and length are set to 1 m. Again a very good agreement is found between FEM and SEA+ calculation (see Figure **7**, Modal density comparison with PSOLID2 model).

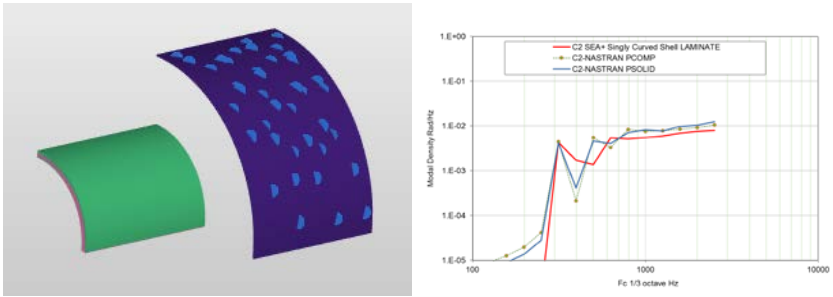


Figure 7. Case C2 - Comparisons of SEA+ and NASTRAN PSOLID2 Model density for a quarter of simply-supported cylinder

### 6.4 Sandwich steel plate with viscoelastic insertion

Case C3 is also a 3-layered steel panel with very thin film of viscoelastic material bonding together two thin steel plates. A sample from ThyssenKrupp manufacturer was measured to compare with SEA+ simulation. Characteristic used in the modeling are reported in next Table 1.

| Manufacturer | Panel size | Skin thickness | Core thickness | Core Young's modulus | Shear modulus | DLF core | Skin Mat. |
|---|---|---|---|---|---|---|---|
| ThyssenKrupp | 0.275m x .2m | 0.75 mm | 0.04 mm | 50 MPa | 40 MPa | 1 | Steel |

Table 2. Characteristic of tested samples

Core material intrinsic DLF is taken equal to 1. Skin DLF are fixed arbitrarily to 0.01.
Regarding measured data, a set of complex frequency transfer inertances were recorded under impact hammer using InterAC SEA-XP data Acquisition system. Driving point inertances are converted into conductance per 1/3rd octave band. Reverberation time on free-free panels is also analyzed and converted into DLF.
In Figure **8** are reported calculated flexural input conductances for both SEA+ and FEM (here PCOMP model result) and measurement. SEA+ modal density and conductances are also found in good agreement with PCOMP, PSOLID and measurement results. Prediction of DLF is also satisfactory compared to measurement as the impact pulse is very short with low modal density below 1000 Hz. Nevertheless, both Power Injected Method (PIM) and Reverberation time are leading to same measured DLF values in the range 200-2000 Hz.

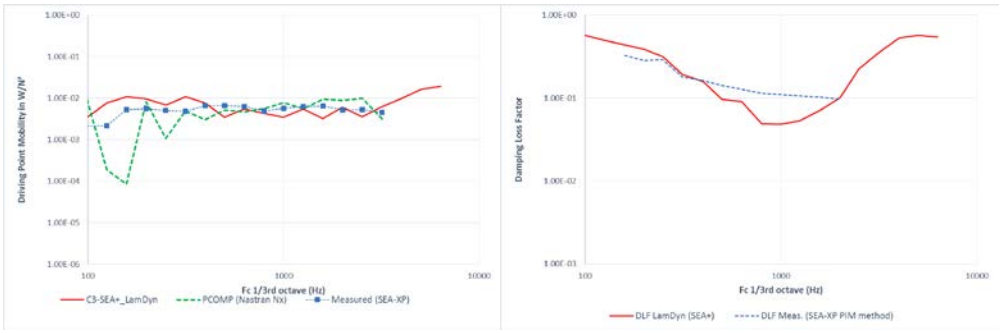


Figure 8. Case C3 - Viscoelastic steel sandwich - **Left**: SEA+ Laminate and NASTRAN PSOLID conductances compared to measurement - **Right**: SEA+ DLF laminate calculation compared to measurement through injected power

### 6.5 Multilayered window

Case C4 is a window made of five layers. Layers are 8mm-Glass, 9.6mm-PU (Polyurethane), 8mm-Glass, 2mm-PVB (Polyvinyl Butyral) and 3mm-Glass. Window size is 0.76m x 1m. Modal density of corresponding SEA+ laminate model is checked against measured and calculated data in Figure **9** (left). Measured modal density is obtained from FRF measurements performed directly on the built-up window with hammer impact. Measured modal density is obtained from the relationship $N = 4mY$ , with $m$ the window mass and $Y$ the real part of driving point FRF. The comparative calculated modal density is extracted from NASTRAN NX FEM model of the window built with PSOLID elements. There is good convergence between the three results taking note that actual window was connected to the mounting frame during the measurement, explaining observed difference at low frequencies between measured and calculated modal densities.

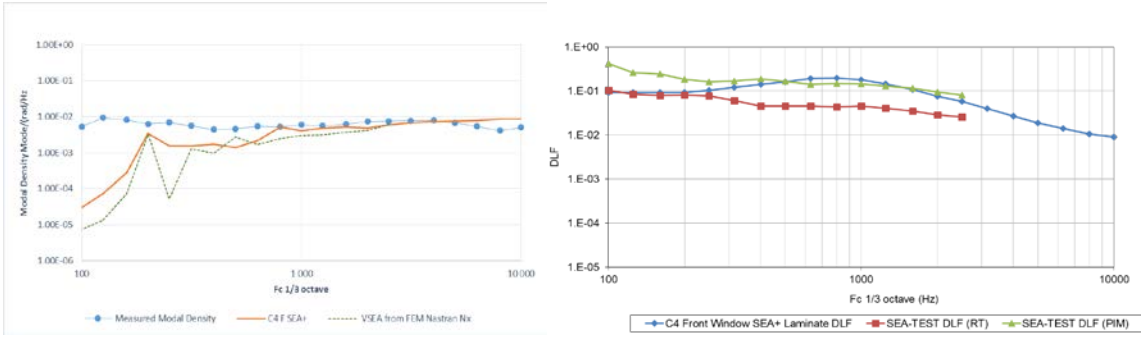


Figure 9. Case C4 - Multilayered window - **Left**: SEA+ and NASTRAN FEM calculated modal density compared with experimental modal density and **Right**: calculated DLF compared with RTIR and PIM measurements

Predicted SEA+ DLF is compared to measured DLF in Figure **9** (right).
Measured DLF is identified in two different ways by Reverberation Time of window Impulse Response (RTIR) and by Power Injected Method (PIM) using SEA-TEST software.

## 7 CONCLUSIONS

The SEA+ Dynamic Laminate model is based on a new theory which provides fast calculation of SEA parameters. This theory is reducing the 3D dynamic of a multi-layered thin shell to the assembly of series of thin orthotropic layers, each layer being described by a single material and by its asymptotic uncoupled dynamic stiffness. Along transverse direction, the strain shape motion is assumed to behave as static with continuous displacement and rotation and discontinuous second z-derivative at layer interfaces. This theory is then a specific instance of the Zig-Zag theory using local asymptotic motions of individual layers in place of the classical Taylor's series decomposition of the global motion for projecting the actual motion. Dynamic Laminate theory has been extended from plate to singly-curved and doubly-curved systems and released in SEA+ 2015. Comparative calculations with FEM models and with measurements have shown good convergence in all tested configurations which were requiring specific SEA model, now all covered by the Dynamic Laminate construction.

## REFERENCES

[1] G. Borello (InterAC), L. Gagliardini, L. Houillon (PSA), L. Petrinelli (Geci Systems). Virtual SEA: mid-frequency structure-borne noise modeling based on Finite Element Analysis. *SAE Noise and Vibration Conference* – May 6-8, 2003 – Traverse City, Michigan, USA.

[2] G. Borello, A. Courjal, R. Nguyen Van Lan (InterAC). Combining Finite Element and SEA approach in Vibroacoustic Analysis. *7th French Acoustic Congress* – March 22-25, 2004 – Strasbourg, France.

[3] G. Borello (InterAC), L. Gagliardini, L. Houillon (PSA), L. Petrinelli (Geci Systems). Virtual SEA-FEA-based Modeling of Structure-Borne Noise. *Sound and Vibration Magazine* – January 2005.

[4] G. Borello, A. Courjal, R. Nguyen Van Lan (InterAC), Analysing structure borne sound transmission in car body using combined FE/SEA techniques. *SIAT* – January 19-22, 2005 – Pune, India.

[5] G. Borello (InterAC), J.-L. Kouyoumji (CTBA). Vibroacoustic Analysis of Sound Transmission in Double-glass Timber Windows. *Inter-Noise* – August 7-10, 2005 – Rio de Janeiro, Brazil.

[6] Luciano Demasi (San Diego University). An invariant Model for any Composite Plate Theory and FEM Applications: the Generalized Unified Formulation. *50$^{th}$ AIAA/ASME/ASCE/AHS/ASC Structures, Structural Dynamics and Material Conference* 17$^{th}$. 4-7 May 2009, Palm Springs, CA, USA.

[7] J.-M. Berthelot. Matériaux Composites, comportement mécanique et analyse des structures. *Masson 2$^{me}$ édition*, 1996.